PHILOSOPHICAL TRANSACTIONS A

royalsocietypublishing.org/journal/rsta

Research

Cite this article: Dumont D. 2022 Marginal ice zone dynamics: history, definitions and research perspectives. *Phil. Trans. R. Soc. A* **380**: 20210253.
https://doi.org/10.1098/rsta.2021.0253

Received: 28 March 2022
Accepted: 10 July 2022

One contribution of 17 to a theme issue 'Theory, modelling and observations of marginal ice zone dynamics: multidisciplinary perspectives and outlooks'.

Subject Areas:
oceanography, glaciology, materials science, applied mathematics, fluid mechanics, wave motion

Keywords:
marginal ice zone, rheology, granular, floe size

Author for correspondence:
Dany Dumont
e-mail: dany_dumont@uqar.ca

Marginal ice zone dynamics: history, definitions and research perspectives

Dany Dumont

Institut des sciences de la mer de Rimouski (ISMER), Université du Québec à Rimouski, Rimouski, QC, Canada G5L 3A1

DD, 0000-0003-4107-1799

Despite enormous scientific and technological progress in numerical weather and climate prediction, sea ice still remains unreliably predicted by models, both in short-term forecasting and climate projection applications. The total ice extent in both hemispheres is tied to the location of the ice edge, and consequently to what happens in the portion of the ice cover immediately adjacent to the open ocean that is called the marginal ice zone (MIZ). There is mounting evidence that processes occurring in the MIZ might play an important role in the polar climate of both hemispheres, yet some key physical processes are still missing in models. As sea ice models developed for climate studies are increasingly used for operational forecasting, the missing physics also impede short-term sea ice prediction skills. This paper is a mini-review that provides a historical perspective on how MIZ research has progressed since the 1970s, with a focus on the fundamental importance of the interactions between sea ice and surface gravity waves on sea ice dynamics. Completeness is not achieved, as the body of literature is huge, scattered and rapidly growing, but the intention is to inform future collaborative research efforts to improve our understanding and predictive capabilities of sea ice dynamics in the MIZ.

This article is part of the theme issue 'Theory, modelling and observations of marginal ice zone dynamics: multidisciplinary perspectives and outlooks'.

THE ROYAL SOCIETY PUBLISHING

1. Introduction

Sea ice is a critically important element of Earth's climate. It modulates the exchanges of heat, mass and momentum between the atmosphere and the ocean through a number of feedback loops involving highly nonlinear coupled processes. The ice cover extent and volume in the Arctic have been decreasing steadily over the past four decades, while it remained fairly stable in the Southern Ocean. Sea ice also constitutes a habitat for multiple species, a hazard for navigation and, in the Arctic, at the very least an essential transportation means for communities. Predicting the behaviour, motion, deformation and evolution of sea ice is particularly challenging at all scales. Climate models were deemed too conservative in their prediction of an ice-free Arctic, and decision-making currently relies on other methods based on observations [1]. Despite the fact that most climate models of the fifth and sixth phase of the Coupled Model Intercomparison Project (CMIP) agree that the Arctic summer sea ice extent will undergo a sustained negative trend, there is significant variability between them as well as large biases compared to available long-term observational datasets [2]. Moreover, there is no consensus in the scientific literature on the cause of such a spread between models [3,4]. For short-term applications, sea ice charts provided by national ice services are still preferred by navigators over model sea ice forecasts provided by today's most sophisticated operational forecasting systems. According to Lemieux *et al.* [5], sea ice forecasting is still in its infancy compared to weather and ocean prediction. A significant part of the uncertainty comes from the difficulty in modelling the transition zone between the ice and the open ocean, referred to as the marginal ice zone (MIZ). Even though sea ice models *cover* this zone, in the geographical sense, they do not account for processes that define it, and doing so is unfortunately not straightforward. A short historical overview certainly helps to understand why.

The development of sea ice models advanced thanks the outstanding impetus of the Arctic Ice Dynamics Joint Experiment (AIDJEX) in the 1970s, during which an international community of experts supported by significant investments was committed to building a sea ice model for climate studies. Research on MIZ dynamics never benefited from such a coordinated effort. Instead, projects like the Marginal Ice Zone Experiment (MIZEX) [6], the Norwegian Remote Sensing Experiment (NORSEX) [7] and the Labrador Ice Margin Experiment (LIMEX) [8] contributed to gather in situ and remote sensing data and acquire important knowledge about the MIZ that fuelled research in many disciplines (wave and sea ice physics and mathematics, material science and engineering, oceanography, remote sensing). Like in many environmental research areas, advances in our understanding of processes progresses along with technological development (more powerful computers, more accessible and higher resolution remote sensing data, new instruments), but also and most importantly, along with interdisciplinary collaboration and integration. Today's understanding of MIZ dynamics is built on the progressive aggregation of different research paths or topics that evolved rather independently and that are currently being integrated.

The first research path was mostly driven by oceanographers and sea ice modellers who viewed the MIZ as *a region where the ice-ocean interactions were intensified, highly variable and complex thanks to an ice pack that has lost its strength and that has undergone substantial changes of its geometrical properties* [9]. This definition does not recognize explicitly the role ocean gravity waves play in shaping the morphological properties of the ice nor on forces they might apply on it. Instead, the focus was placed on the ocean response near the ice edge with respect to mesoscale circulation and its influence on vertical fluxes of heat, salt and biogeochemical tracers, but also on the formation of dense water. As we approach the ice edge and the open ocean limit of the MIZ, the ice is free to move in response to external forces. In these free drift conditions, wind stress drives sea ice more efficiently than the current, such that sea ice often moves faster than the current [10,11], leading to a more efficient transfer of momentum from the atmosphere to the ocean. Numerous studies investigated the various ramifications of this problem that are presented and discussed in §2.

The second path aimed at understanding wave–ice interactions, particularly how waves propagate in an undeformed uniform floating ice sheet, and in a sea covered by multiple ice

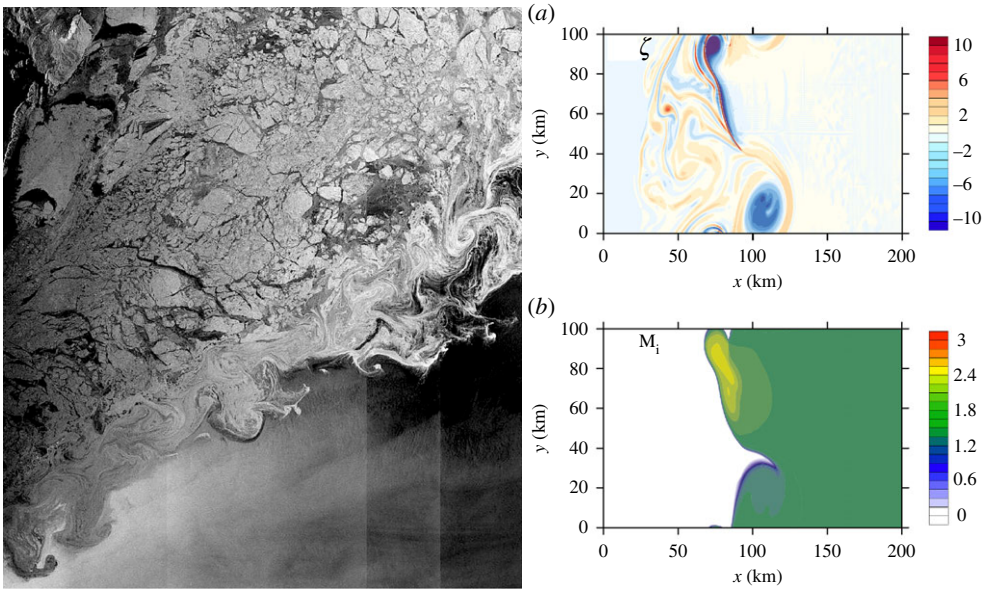

Figure 1. On the left, a synthetic aperture radar (SAR) image of Fram Strait on 16 January 2010. The east coast of Greenland is visible on the top left and the open ocean in the bottom right of the image. To the right, the relative vorticity field (10^{-5} s^{-1}) showing eddying activity (*a*) and the ice mass (m) around the ice edge (*b*) resulting from a coupled wave–ice-ocean idealized model of the MIZ, reproduced with permission from [16], their figure 7. (Online version in colour.)

fragments of different sizes, shapes and arrangements. The vast scientific literature on this subject was not always intended to apply to the MIZ, but also to other problems or phenomena related to landfast ice, ice islands and icebergs, coastal infrastructures and offshore engineering. The development of mathematical solutions to a hierarchy of problems representing waves propagating in sea ice and in the MIZ have been carefully reviewed in the past [12–14]. Recently, the research focus has moved towards resolving how momentum and energy is transferred between the wind, waves and the ocean in the presence of various sea ice conditions. This topic is reviewed by Jim Thompson in this issue [15].

The third path focuses on deriving rheology that is suitable for the MIZ. Since the MIZ is traditionally defined as the area where concentration is low (below 80%) sea ice is often considered to be in free drift, i.e. where ice motion results from the equilibrium of external forces like winds and currents. However, the MIZ can also be made of ice floes closely packed against each other, with frazil in between such that individual floes are not freely drifting. Such an ice jumble is also very distinct from a large consolidated ice sheet that would either behave as an undeformed solid, or fracture, fail and deform like plastic or brittle material. Figure 1 (left panel) shows a synthetic aperture radar (SAR) image of sea ice in Fram Strait that illustrates quite clearly the very distinct response of the ice to stresses in the MIZ adjacent to the open ocean, compared to the ice pack inward [17]. Unfortunately, there were only very few attempts to derive such rheology and there is virtually no existing dataset so far that would inform and validate such a rheology. In this issue, Agnieszka Herman provides a review and a contemporary view on how to derive a physically adequate rheology for the MIZ [18]. Here, in §3a, I will instead describe the most commonly used sea ice rheology for geophysical applications, and discuss how it could be modified in order to become applicable to sea ice in all conditions, including the MIZ.

The fourth and last path concerns wave-induced ice break-up, and more generally how the floe size distribution (FSD) evolves in response to numerous processes. The FSD constitutes an important link between waves and the behaviour of fragmented ice that is currently missing in models. Plastic failure in sea ice can break-up very large sheets of ice into smaller pieces

such that floe size typically adopts scale-independent power law distributions [19,20]. However, wave-induced fracture can transform the ice cover into a slurry composed of small fragments interspersed with slush or brash ice. A short discussion about the recent research on wave-induced ice break-up is presented in §3a as a key component of coupled wave–ice models, but I refer the reader to the review on the FSD and related concepts by Chris Horvat in this issue [21].

It is only during the last decade or so that these research paths really started to converge. Recognizing that this mini-review cannot be complete, as the body of literature is huge, scattered and rapidly growing, we structure it into two parts. The first part seeks a definition of the MIZ in a dynamical perspective (§2) while the second one reviews and discuss MIZ dynamics from a sea ice perspective by reviewing and discussing the momentum balance equations for sea ice (§3), emphasizing two terms: the rheology and the wave radiative stress. A conclusion is provided in §4.

2. Defining the marginal ice zone and posing the problem

The MIZ bears many definitions owing to the angle with which one regards it. Broadly, it identifies the region located at the margins of the main ice cover of the Arctic Ocean or surrounding Antarctica. The observed variable that is traditionally used to assess the variability and trends of ice edge position and MIZ extents in both hemispheres is the sea ice concentration (SIC) obtained from passive microwave satellite remote sensors that provide a global coverage since 1979. The most widely used operational definition of the MIZ is the area of the ice-covered ocean that is adjacent to the open ocean and where the ice concentration is less than 80% and more than 15%. Using this definition, Strong and Rigor [22] found that over the period 1979–2011, the summer (July–September) Arctic MIZ width increased by 13 km decade^{-1}, which corresponds to a 39% widening. A similar analysis carried out recently for the period 1978–2018 found no clear trend in MIZ extent [23] and authors called for caution when interpreting such results. Methods based on SIC criteria have also been used to study the Antarctic MIZ and polynyas [24,25]. Although these definitions may be appropriate in some contexts (primary production, marine ecosystem dynamics, ship navigation, model skill assessments, etc.), they do not inform very well about MIZ dynamics and how it may affect atmosphere-ice-ocean exchanges and the climate.

To better understand how the MIZ works and seek more representative definitions, let us look again at the left panel of figure 1. Visually, one can distinguish remarkable differences between sea ice that is near the ice edge and sea ice in the inner drifting pack. Ice floes in the MIZ are of the order ($\mathcal{O}10^2$ m), while the central part is made of very large floes ($\mathcal{O}10^3 - 10^5$ m) separated from each other by so-called linear kinematic features (LKF) indicative of shear or divergence. Inversely, patterns in the MIZ follow vortical motion, eddies, fronts and filaments, indicative of ocean turbulence at the meso and submesoscale. We also see that sea ice concentration is not significantly lower in the MIZ compared to the inner pack, and is sometimes even higher in some areas. This image nicely represents the problem that was addressed by many authors since the late 1970s, at the beginning of the satellite era. Basically, they tried to understand the mechanisms responsible for the observed vorticity and to determine what role sea ice plays in this.

Three mechanisms are generally invoked to explain the formation of submesoscale and mesoscale motions in the MIZ [16]. The first mechanism is not directly linked to sea ice but may impact sea ice in some MIZs, and involves the perturbation of the flow vorticity due to changes in the bathymetry [26]. The two other mechanisms are directly linked to fact that the wind transfers momentum to the ocean more efficiently when there is drifting sea ice than in the open ocean. First, a uniform wind blowing over a meandering ice edge, or over a straight edge with non-uniform sea ice concentration, produces a wind stress curl that input relative vorticity to the flow field, thus generating eddies to which are associated zones of upwelling and downwelling [27,28]. Second, eddies can arise from barotropic or baroclinic instabilities when wind-driven ocean surface currents are amplified by the presence of ice [29]. The role of waves in this problem was first studied by Liu *et al.* [30] who found that the wave radiation stress acts to sharpen ice edges and enhances wind stress and thus amplifies the formation of eddies and the associated

baroclinic response of the ocean, thus contributing to the two last mechanisms. This problem was revisited by Dai *et al.* [11,16] with a more sophisticated wave–ice-ocean modelling framework. Figure 1*a*,*b* shows the flow vorticity and the ice mass (proportional to thickness) resulting only from waves at a slightly oblique incidence with respect to the ice edge, clearly demonstrating the non-negligible role of waves in shaping the MIZ. The wave radiation stress in described and further discussed in §3b.

The idea that waves fundamentally define MIZ dynamics has been reinforced by the advent of high resolution SAR remote sensing and improved signal processing methods [31] that allowed seeing and measuring waves-in-ice. Figure 2 shows a nice example of that in the MIZ of Fram Strait on 5 October 2014. The top panel shows the full transition between the open ocean, through the MIZ into the interior ice pack. Waves are visible in the open ocean, but appear even clearer in the MIZ. They propagate until they disappear right where floes appear much larger. The lower panel shows a close-up of the top panel where waves are breaking-up a 15 km large floe into much smaller ones.

Based on this brief overview, there seem to be a few avenues that could lead to a systematic characterization of the MIZ at the global scale and that are representative of its dynamics using satellite remote sensing. A first avenue would take advantage of the distinct kinematic features that characterize the inner ice pack (LKFs, large floes) and the MIZ (mesoscale turbulence, small floes) and involve the development of pattern recognition methods optimized for the MIZs (e.g. [32]). This method has to my knowledge never been developed or implemented.

A second avenue is the extent to which waves propagate in sea ice. Methods for extracting waves height and wave attenuation from SAR imagery have been developed and used with Seasat [33], with the European Remote Sensing Satellite 2 (ERS2) [34] and more recently with the higher resolution wave mode imagery of Sentinel-1 [35,36] from which the directional wave spectrum can be obtained as well as information about wave attenuation. As demonstrated recently, wave parameters can also be obtained from ICESat2 altimeter data, a satellite mission launched in 2018 [37,38].

A third avenue is through the direct measurement of floe size or the FSD. Again, pattern recognition algorithms could be developed and applied to SAR images [39,40]. Ice charts produced by national ice services of circumpolar countries for some Arctic regions contain information about the *form of ice*, which is a visual assessment of the dominant floe size inside a certain area having similar ice characteristics. The National Ice Center produces ice charts for the Antarctic, but they do not include information about floe size. Ice charts are essentially polygons drawn by ice specialists who interpret satellite or aerial images and determine ice conditions using a standard method called the egg code [41]. Figure 3 shows how the information contained in ice charts can be used to estimate a significant MIZ width over a given region. First, polygons are selected using a criterion for the MIZ. In the egg code, CT is the total concentration in tenths (1 to 10) and FA is the floe size category going from X (no floe) to 10 (giant floes >10 km). Knowing that wave-induced fracture produces floes that are smaller than $\sim 200 - 500$ m [42], all polygons adjacent to the open ocean with FA ≤ 4, which corresponds to floes smaller than 500 m, can be tagged as the MIZ. Once polygons are selected, they are merged and the significant width is obtained by averaging the Euclidean distance along the skeleton of the irregular elongated shape along forming the MIZ (figure 3*a*–*d*). In Fram Strait, the seasonal variation of the width of MIZ correlates well with the seasonal variations of wind and wave intensity (red line in figure 3*e*), whereas a MIZ defined using a concentration threshold (CT ≤ 8) is much wider during the melt season and when winds are calmer.

We can thus suggest three definitions for the MIZ that are or could be applied operationally to satellite remote sensing data to better inform MIZ dynamics: (i) sea ice displaying vortical motions, with a threshold to be determined, (ii) sea ice in wavy motion and (iii) sea ice with a dominant floe size less than a upper value (in the order of 200–500 m).

These three definitions each reveal different aspects of MIZ dynamics. They could be use to build datasets long-term and near-real-time datasets against which model development could be informed, tested and validated. The next section reviews the knowledge about how waves and

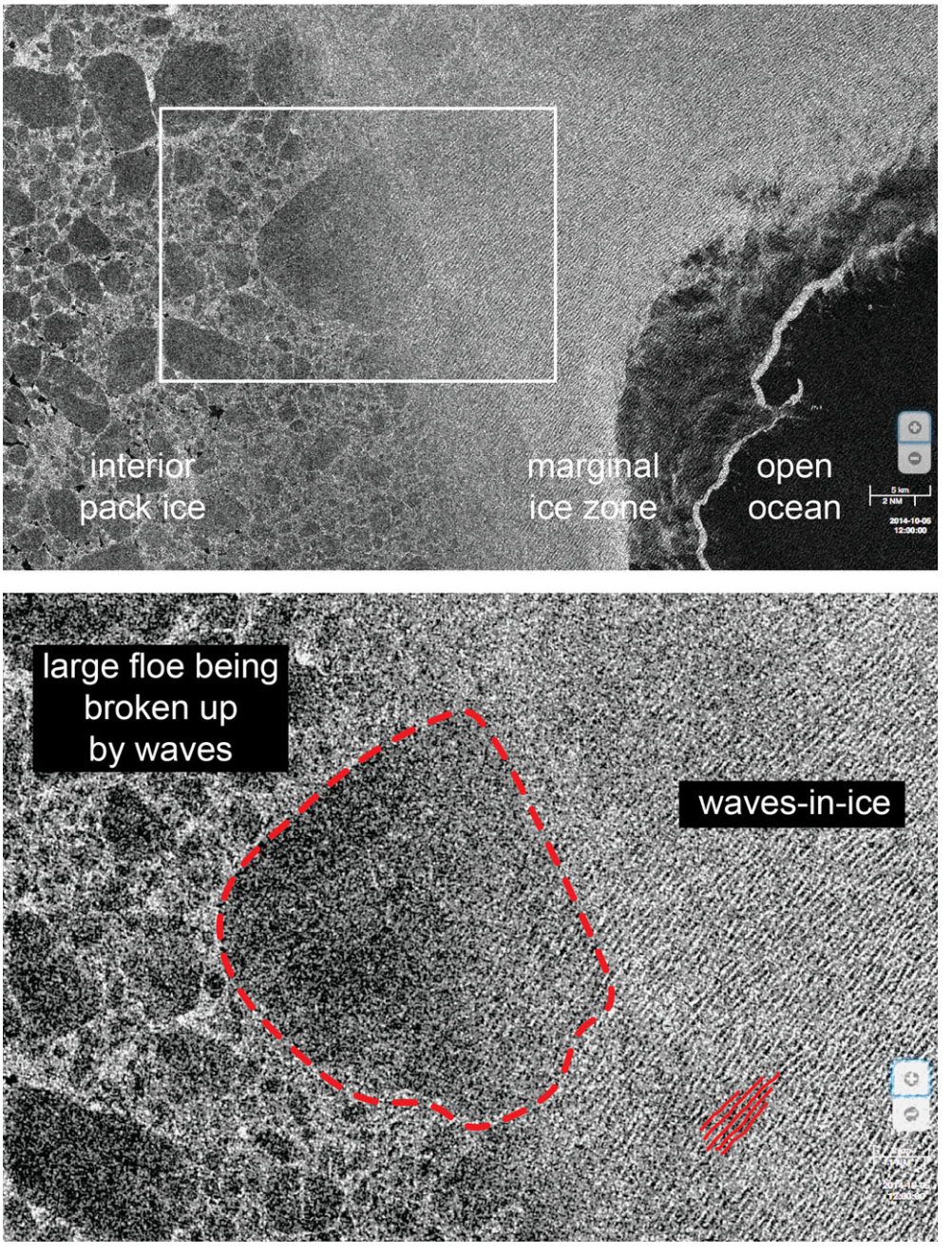

Figure 2. Sentinel-1 image of the marginal ice zone in Fram Strait (4.54° E, 80.76° N) on 5 October 2014 15:04:47 UTC extracted from the SWARP portal (https://swarp.oceandatalab.com/). (Online version in colour.)

floe size impact sea ice dynamics by recalling the basic momentum and mass balance equations that are at the base of state-of-the-art and emergent models.

3. Sea ice momentum and mass balance equations

The foundations of today's general understanding and models of sea ice dynamics were laid in the 1970s during and after the AIDJEX (see [43] for a review). The goal of this major field experiment initiative carried out in 1975 and 1976 on the central Arctic ice pack, more specifically

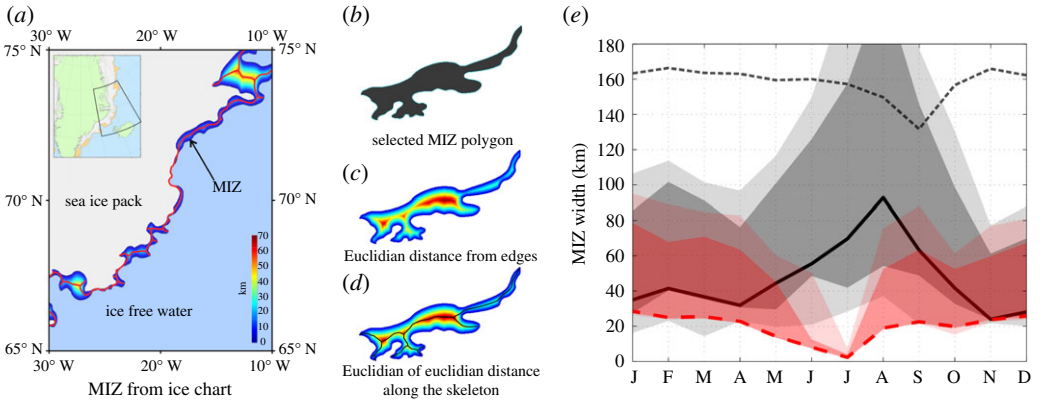

Figure 3. A method for estimating the average width of the MIZ using information about floe size from World Meteorological Organization (WMO) SIGRID-3 ice charts produced for navigation in Arctic waters. Ice charts are interpretations of aerial and satellite images made of polygons having similar sea ice properties (concentration, thickness and floe size) synthesized with the egg code. First, polygons satisfying the criterion are selected in the ice chart (*a*,*b*), the Euclidian distance from edges is computed for each polygon (*c*) and values along the skeleton are averaged (*d*). Panel (*e*) shows the seasonal variations of the MIZ defined with a concentration threshold (total ice concentration less than 80%, or CT $\leq$ 8, black soliid line) and with a floe size criterion (dominant floe size less than 500 m, or FA $\leq$ 4, red dashed line) in the southern Fram Strait area (rectangle in the inset map). The black dotted line indicates the total ice extent from the coast of Greenland. Solid and dashed ines indicate the 12-year average, while shaded areas represent the 25th and 75th (dark shaded areas) and the extrema (light shaded areas). (Online version in colour.)

in the Beaufort Sea, was to collect a comprehensive dataset of how sea ice moves and deforms in response to oceanic and atmospheric forces. Indeed, it was recognized that thermodynamics alone cannot explain the large-scale aerial extent and ice thickness distribution (ITD). The experiment focused on constraining the various terms of the momentum balance equation for sea ice in order to eventually come up with a model formulation suitable for inclusion in global climate models. It led subsequently to a much better representation of the ice-albedo feedback and freshwater fluxes in climate models, two first-order climate drivers in the Arctic with global repercussions. Roughly 40 years later, the basic equations describing sea ice dynamics in contemporary models have remained very similar to their original formulations, with somewhat minor sophistications aimed at improving the computational efficiency. However, substantial modifications are needed in order to better account for wave–ice interactions and to represent MIZ dynamics adequately. I recall here the basic equations that are used today with an emphasis on terms that are affected by oceans waves and wave–ice interactions.

The momentum balance equation for sea ice that is generally used in most contemporary models considers sea ice as a two-dimensional continuum floating on the ocean and is expressed as [5]

$$\rho_i h \left(\frac{\mathrm{D}\mathbf{u}}{\mathrm{D}t} + \mathbf{f} \times \mathbf{u} \right) = \mathbf{F}_i + \nabla \cdot \boldsymbol{\sigma} \tag{3.1}$$

in units of Pa or N m^{-2}. The two terms on the left represent the total acceleration in a rotating frame of reference, where $\mathbf{u} = u\hat{\mathbf{i}} + v\hat{\mathbf{j}}$ is the horizontal sea ice velocity vector, ρ_i is the ice density, h is the mean ice thickness, and $\mathbf{f} = f\hat{\mathbf{k}}$ is the Coriolis parameter. Equations are written in Cartesian coordinates where $\hat{\mathbf{i}}$, $\hat{\mathbf{j}}$ and $\hat{\mathbf{k}}$ are unit vectors aligned with the x, y and z axes, respectively. Note that the actual thickness of ice present in a grid cell is h/A, where A the total area fraction covered with ice. In multi-category models, the ice thickness is represented as an ice ITD $g(h)$, which is presented later. The second term is on the right-hand side of equation (3.1), $\nabla \cdot \boldsymbol{\sigma}$, is referred to as the rheology term and corresponds to the internal response of the ice to external stresses. The first

term on the right-hand side $\mathbf{F}_i$ represents the external forces acting on the ice. The most general and complete form of this term is given by

$$\mathbf{F}_i = \boldsymbol{\tau}_g + \boldsymbol{\tau}_a + \boldsymbol{\tau}_o + \boldsymbol{\tau}_b + \boldsymbol{\tau}_w. \tag{3.2}$$

In addition to the terms on the left-hand side of equation (3.1), the three first terms on the right-hand side of equation (3.2) are those that were specifically considered by the AIDJEX group. The first one is the gravity pull on a tilted ocean surface, which is expressed as $\boldsymbol{\tau}_g = -\rho_i g_e \nabla H$. Here, g_e is the gravitational acceleration, and H is sea level elevation above the mean. The two other AIDJEX terms are the tangential forces exerted by the wind and ocean currents, respectively, expressed as $\boldsymbol{\tau}_a = \rho_a C_{da} A|\mathbf{u}_a - \mathbf{u}|(\mathbf{u}_a - \mathbf{u})$ and $\boldsymbol{\tau}_o = \rho C_{do} A|\mathbf{u}_o - \mathbf{u}|(\mathbf{u}_o - \mathbf{u})$, where ρ and ρ_a are the water and air densities, C_{da} and C_{do} are the air-ice and ocean-ice skin drag coefficients, and $\mathbf{u}_a$ and $\mathbf{u}_o$ are wind and current velocity right above and beneath the ice. Those expressions have not evolved much and refinements have been proposed mostly for the parameterizations of drag coefficients, to better account for roughness both above and below sea ice [44–46]. The fourth term of equation (3.2) represents interactions between the ice and the seabed when ice ridge keels are deep enough or when tidal oscillations are large enough that the ice lies on the ground in shallow waters [47]. It does not generally apply to the MIZ, but is given here for completeness. The last term of equation (3.2) is, however, crucial and has been added to sea ice models only very recently for investigating its effects on MIZ dynamics. This force, noted $\boldsymbol{\tau}_w$, represents the push exerted by surface gravity waves as they attenuate (see §3b).

In addition to the momentum balance, a mass balance equation is needed in order to adequately account for drift, deformation and morphological changes of sea ice. It is based on the concept of ice ITD noted $g(h)$, which is one of the major legacies of AIDJEX and was introduced by [48]. It is defined such that $g(h)\,\mathrm{d}h$ is the area fraction covered by ice with thickness between h and $h + \mathrm{d}h$ at time t in a given model grid cell. It is thus a function of space, time and thickness that obeys the following differential equation

$$\frac{\partial g}{\partial t} = -\nabla \cdot g\mathbf{u} + \psi + \frac{\partial F g}{\partial h} + L. \tag{3.3}$$

In numerical sea ice models, $g(h)$ is generally discretized in a finite number of thickness categories, typically 5 to 10. The first term of equation (3.3) represents the horizontal transport, while the second term ψ determines how sea ice thickens during convergence in order to ensure the conservation of sea ice volume. This is often called the thickness redistribution [48]. The third term represents changes to the distribution of thickness due to ice melt and growth, and also how snow transforms into sea ice, where F results from a vertical one-dimensional thermodynamics model often discretized in many levels in ice and snow. The last term noted L accounts for the additional area of ice in contact with the ocean when that is a function of the average floe size [48,49]. This is the only connection between sea ice dynamics and floe size that there was until recently. Floe size and its space–time evolution has been introduced for the first time by [50], but it is Horvat & Tziperman [51] who first formally generalized equation (3.3) to account for the evolution of floe size as a key state variable for describing sea ice at the subgrid-scale. The ITD becomes in this context a floe size and thickness distribution (FSTD) noted $J(r,h) = J(\mathbf{r})$, where r is used here as a variable representing a horizontal scale of floes and not strictly the radius of a disk. The most general expression for its evolution is [51]

$$\frac{\partial J}{\partial t} = -\nabla \cdot J\mathbf{u} + (\mathcal{L}_M + \mathcal{L}_T + \mathcal{L}_W)J, \tag{3.4}$$

where $\mathcal{L}_M$, $\mathcal{L}_T$ and $\mathcal{L}_W$ are, respectively, the mechanical redistribution due to ridging or rafting that affect both floe size and thickness, the thermal processes affecting floe size and thickness and the wave-induced break-up. This last term is generally expressed as

$$\mathcal{L}_W(r,h) = -Q(r,h) + \int_0^\infty Q(r',h)\beta(r,r',h)\,\mathrm{d}r', \tag{3.5}$$

where $Q(r,h)$ is the rate at which floes of size r and thickness h breaks and $\beta(r,r',h)$ is a function that tells the sizes of floe fragments when a floe of size r' breaks up. Again, observations of wave-induced break-up of sea ice in the natural environment that would be useful to inform these functions are very rare. There are two known studies, one involving freshwater ice in the laboratory [52] and one where a ship is used to generate waves that break-up natural sea ice [53].

The FSTD provides the necessary handle for coupling sea ice and wave models that could determine prognostically how morphological properties of sea ice evolve, and thus a way to represent when and where MIZ dynamics should apply. Floe size is thought to affect melt rate by exposing more surface of the ice to the ocean, and according to modelling studies, this effect can be significant, especially when floes are ~30 m and smaller [49] and can interfere with other processes in setting up the ITD [54]. However, these conclusions are not yet supported by observational evidence. An attempt was made during MIZEX using photogrammetry to quantify this effect in the field [55], but results were deemed inconclusive. Floe size can also strongly control shear and compressive strength, as is discussed below, such that floe size and waves-in-ice are indeed more appropriate indicators for the MIZ than concentration can be [17].

(a) Rheology

One major legacy of AIDJEX was to consider sea ice as a plastic material that does not deform until a critical stress state is reached and that ice irreversibly deforms [43]. Plastic failure refers to the fact that sea ice can resist to external stresses until a limit is reached and that localized and rapid deformation occurs to release the stresses. This behaviour is quite challenging to represent adequately in a numerical modelling framework applicable at geophysical scales. Whether sea ice should be modelled as an elastic, brittle, viscous and/or plastic material was and is still debated today. Nonetheless, the questions whether this apply to the MIZ and how would rheology for the MIZ be obtained and mathematically formulated were never really addressed in a coordinated way. To proceed towards the development of rheology for the MIZ, let us assume on one hand that there exists a formulation that applies to all sea ice conditions, and on the other hand that within the ice pack, the viscous-plastic rheology applies. The latter assumption could apply to another rheology, and the VP is adopted here for simplicity and because it is the most commonly used today. In this section, I thus describe the VP rheology and discuss how it could be modified to better account for the MIZ.

Before presenting its seminal viscous-plastic formulation that is still widely used today [56], Hibler discussed in 1977 how a stochastic plastic behaviour could be formulated as a viscous law in certain limits and considering proper spatial and time scales [57]. Similarly here, we should keep in mind that the way we may decide to represent a process in a geophysical model may not always be representative of how the process works at a smaller scale. Parameterizations are generally developed to simulate an averaged effect of a process at a large scale rather than realistic representing the process itself. Let us recall here the general expression of the second-order internal stress tensor that appears in the last term of equation (3.1) is given by

$$\sigma_{ij} = 2\eta\dot{\varepsilon}_{ij} + (\eta - \zeta)\dot{\varepsilon}_{kk}\delta_{ij} - \frac{p}{2}\delta_{ij}, \tag{3.6}$$

where $p = \frac{1}{2}(\sigma_1 + \sigma_2)$ is the isotropic pressure term, η and ζ are bulk and shear nonlinear viscosities, which generally depend on A, h and strain rates. The stress state can be expressed in terms of principal stress components (σ_1, σ_2) or stress invariants (σ_I, σ_II) corresponding to the mean isotropic pressure and the maximum shear stress, respectively. Similarly, the strain rate is a second-order tensor defined as $\dot{\varepsilon}_{ij} = \frac{1}{2}(\partial_i u_j + \partial_j u_i)$ and also characterized by principal and invariant components. The form of viscosity and ice strength terms depend on prior physical assumptions about the material. The Hibler viscous-plastic rheology that is commonly used for

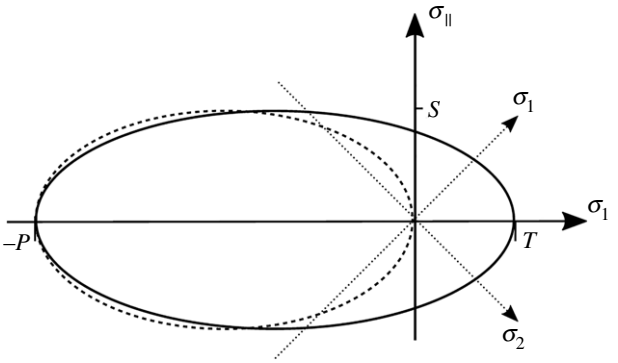

Figure 4. The elliptical yield curve of Hibler's viscous-plastic rheology depicted in the principal (σ_1, σ_2) and invariant (σ_1, $\sigma_{\|}$) stress space, with P the compressive strength, S the shear strength and T the tensile strength of the ice. This is one among numerous yield curves proposed and used in sea ice models. Reproduced with permission from [58], their figure 1*a*.

sea ice have the following parameterizations (see figure 4):

$$P = P^* h\, \mathrm{e}^{-C(1-A)}, \tag{3.7}$$

$$\eta = \frac{4S^2 f(\dot{\varepsilon})}{(P+T)} \tag{3.8}$$

and

$$\zeta = (P+T) f(\dot{\varepsilon}), \tag{3.9}$$

where $f(\dot{\varepsilon})$ determines the exact form of the yield curve. P is the compressive strength of the ice, i.e. the maximum isotropic pressure it can sustain before it fails and starts converging and thickening. Many types of yield curves have been proposed and are used in models but none include a dependence on floe size, while the shape and size of grains are known to affect rheological properties of granular materials. The effects can be quite significant, as argued previously. One extreme example is when landfast ice is broken-up by waves [59,60]. In such cases, sea ice transitions from a static solid state to a drifting state under the same external forcings. The parameterization of rheological quantities as a function of floe size is yet to be done for sea ice.

The first and very few attempts to develop a rheology applicable to the MIZ considered the collisional model where a large number of solid disks having a finite diameter d that is small compared to the strain $\dot{\varepsilon}$ are agitated by waves [61,62] such that their random fluctuation velocity $v' \gg \dot{\varepsilon} d$. One intrinsic challenge for crafting a constitutive relation for granular materials is that depending on conditions, they can behave as a solid, a liquid or a gas [63]. The analytical equations derived by Shen *et al.* [62] for the collisional rheology from a number of assumptions were representative of a granular gas, which does not apply well to a dissipative MIZ. The theoretical work of Feltham [64] used the concept of granular temperature to derive a collisional rheology, where the wind turbulence was the main source of kinetic energy causing floe–floe interactions [64]. The applicability of these models to the wide range of conditions characterizing the MIZ was rather limited.

Even though there were very few other rheology models suitable to the MIZ, research aimed at finding constitutive relations for granular materials remained fairly active. Herman [18], in this issue, presents a review of collisional rheologies and more generally granular effects in the MIZ. She also carries out thorough sensitivity analyses of the friction coefficient as a function of FSD for a dense granular flow rheology using a discrete-element modelling (DEM) approach. The dependence of the friction coefficient on the shear rate appears as a very robust feature of the sea ice response to external stresses, which is not the case in the viscous-plastic and

collisional rheologies. Even though DEM are not suitable for direct implementation in two-dimensional continuum models, they can be useful to study emergent averaged properties from which parameterizations can be developed.

(b) Wave radiation stress

Water waves transport momentum and the excess flow of momentum is called wave radiation stress [65]. Following Newton's Second Law, a force is exerted on a medium or a solid body whenever momentum is absorbed or reflected [66]. The wave radiation stress associated to a wave spectrum in its most general form is a second-order tensor given by

$$\mathbf{R} = \rho g \int_0^{\infty} \int_{-\pi}^{\pi} F(k,\theta) \begin{bmatrix} \frac{c_g}{c}\cos^2\theta + \left(\frac{c_g}{c} - \frac{1}{2}\right) & \frac{c_g}{c}\cos\theta\sin\theta \\ \frac{c_g}{c}\cos\theta\sin\theta & \frac{c_g}{c}\sin^2\theta + \left(d\frac{c_g}{c} - \frac{1}{2}\right) \end{bmatrix} k \,\mathrm{d}\theta \,\mathrm{d}k, \tag{3.10}$$

where $F(k,\theta) = F(\mathbf{k})$ is the directional wavenumber spectrum, $\mathbf{k}$ is the wavenumber vector of amplitude k and direction θ, and c and c_g are, respectively, the phase and group speed of wave, that is, a function of $\mathbf{k}$. Note that the terms in brackets are components R_{ij} of a two-dimensional tensor in Cartesian coordinates where θ is the wave propagation angle with respect to the x axis. The force per unit distance that applies to sea ice (fifth term of equation (3.2)), is the divergence of this stress, noted

$$\boldsymbol{\tau}_w = -\nabla \cdot \mathbf{R} = -\frac{\partial R_{ij}}{\partial x_i}\hat{\mathbf{e}}_j. \tag{3.11}$$

In the MIZ, the divergence of the wave radiation stress is dominated by the attenuation of the total wave energy, noted E, which corresponds to the integral overall wave components of the wave energy directional spectrum $\iint F(k,\theta)k \,\mathrm{d}\theta \,\mathrm{d}k$. Assuming an exponential decay of the total wave energy along the x-axis at a damping rate α, such that $E(x) = E_0\,\mathrm{e}^{-\alpha x}$, one obtains that the force applied on the sea ice is given by $\boldsymbol{\tau}_{wx} = \frac{1}{2}\rho g \alpha E_0\,\mathrm{e}^{-\alpha x}$, where E_0 is the incident wave energy before it is absorbed by sea ice. The wave energy attenuation scale α is a fundamental parameter for setting the scale of the MIZ. It has been estimated in many conditions, using various methods, and there is mounting evidence on its complex multivariate dependence. Since a review of how α is estimated is beyond the scope of this paper, I refer the reader to the mini-review of Jim Thompson, in this issue [15].

The radiative wave force can play a significant role in the MIZ and must be included in sea ice models. Here are some examples. Even though it is possible to generate mesoscale eddies with models that do not take ocean waves into account, it has been shown that waves alone can induce a curl in the surface ocean stress, or accelerate a wave-driven current under ice that become unstable [16,30] (see also figure 1). When combined with the wind, waves contribute to sharpen ice edges, which intensifies gradients of momentum transfer and further accelerate currents [16]. The wave radiation stress can also significantly thicken sea ice by compression. During the BicWin field campaign in the St. Lawrence Estuary, Canada, wave spectra and thickness measurements obtained in a stationary MIZ composed of small floes a few metres in diameters and surrounded by slush, were used to constrain an equilibrium model between the wave radiative stress divergence and the ice compressive strength [67]. They used a compressive strength model based on a Mohr-Coulomb criterion and the assumption that gravity (and buoyancy) is the main forcing holding the individual pieces of the ice jumble together, including the slush in between floes that can form an important portion of the ice mass. The compressive strength is given by [68,69]

$$P = \frac{h^2}{2}\rho_i g_e \left(1 - \frac{\rho_i}{\rho}\right)(1-n)\left(\frac{1+\sin\phi}{1-\sin\phi}\right), \tag{3.12}$$

where n is the porosity of the ice jumble and ϕ is the Mohr-Coulomb internal friction angle. Since all parameters are constant except h, this expression is often simplified to $P = h^2 K_r$ [69,70]. It is worth noting that the formulation of the ice compressive strength has been and is still very simply

treated in ice models, although it represents an area of active research [68,69] that is relevant for MIZ dynamics. For instance, the porosity n, often treated as constant, might become an important variable in a realistic MIZ dynamical representation.

Estimations of the wave radiative push from SAR wave data in the Southern Ocean show that the local amplitude of the wave radiation stress can be in the order of 0.01 to 1 Pa depending on incident wave energy and attenuation rates [36], which is not so dissimilar to typical wind stress values. However, the cumulative forces applied to the ice by the waves can be much higher than that of the wind near the ice edge. The main finding was that using their simple equilibrium model, Sutherland & Dumont [67] were able to derive a length scale over which waves dominate the wind

$$L_{\mathrm{MIZ}} = \frac{\rho g_e}{32 \rho_a C_{da}} \left(\frac{H_s}{U_{10}} \right)^2 \tag{3.13}$$

and that can be obtained using only information about the incident significant wave height H_s and wind speed U_{10}. In the Southern Ocean, for example, L_{MIZ} can be as large as 40 km [67]. The other important result is that the wave radiation stress is able to significantly compress and thicken the fragmented sea ice. The equilibrium thickness is of the order

$$h_{\mathrm{eq}}^2 = \frac{\rho g_e H_s^2}{4 K_r} \tag{3.14}$$

and can be of the order of 1–2 m, beyond which the Mohr-Coulomb rheology might not be an appropriate model. Note that equations (3.13) and (3.14) do not reveal the variable nature of the wave radiative push on the ice that depends on sea ice properties. It also assumes that all momentum that is lost by the waves is transferred to the ice, which remains to be confirmed. Instead, they provide integral scales for MIZ length and thickness that highlights the importance of this mechanism.

In order to investigate the relationship effects of the wave radiation stress on an ice edge, Auclair *et al.* [71] (this issue) use a one-dimensional sea ice dynamics model [72] to carry out sensitivity analyses of the ice edge displacement and MIZ thickening to various wave and wind forcings as well as to the wave attenuation function. The authors note that in situ thickness measurements obtained during BicWin can only be reproduced by a model using a compressive strength having a quadratic dependence on thickness, while Hibler's formulation (equation (3.7)) having a linear dependence on thickness was too stiff. The neXtSIM model that is based on an elasto-brittle rheology, used a h^2 dependent strength in its original version [73], while it uses a $h^{3/2}$ dependence in its latest version [74], following the work of Hopkins *et al.* [68,75]. With the h^2 strength, Williams *et al.* [73] obtained only small ice edge displacements caused by the wave radiative stress, but only because the initial sea ice thickness was already 1 m-thick. Those results may have important implications for how we model sea ice in the MIZ. Imagine a situation where thin sea ice is pushed by waves inward at the ice edge up until it reaches 100% concentration, but that this thin ice is too stiff to be further compressed and ridged by waves. Imagine now that this thin ice can thicken up to ∼1 m due to compression by waves. This will move the ice edge inward by $\mathcal{O}(1 - 40\,\mathrm{km})$ and expose the open ocean to the atmosphere where heat exchanges are orders of magnitudes larger. Although affecting only a small portion of the ice cover, the question remains as to what is the cascading effect of modifying the strength on the overall atmosphere-ice-ocean system.

4. Discussion and conclusion

In this review, we highlighted that physical processes happening in the MIZ tightly couple the ocean, sea ice and the atmosphere and that this coupling is strongly mediated by ocean waves. Wave–ice interactions and their impact of MIZ dynamics are well overlooked by numerical models, which is inherited by the challenges associated with collecting data in that area and with the lack (or the late happening) of a coordinated international and inter-disciplinary approach to identify and tackle relevant scientific questions. One overarching question is whether, how

and how much wave–ice interactions matter in the future evolution of sea ice state and climate. Answering this question requires the development of a coupled wave–ice-ocean modelling framework that is informed and validated with relevant and dedicated field studies, as well as the implementation of systematic observational products of MIZ dynamics. Efforts in this direction are well underway with the recent development of coupled wave–ice models [76] and remote sensing products of waves-in-ice [37,38] and floe size [77]. This review further highlights a number of specific questions and research avenues that are summarized below:

— A generalized rheological model should be applicable to any type of sea ice in both hemispheres. The joint FSTD and wave parameters are pivotal prognostic variables that require the coupling of wave and sea ice models. How do ice strength and viscosities (in shear and compression) depend on floe size, porosity, frazil fraction and possibly on wave agitation?
— Wave propagation and attenuation in sea ice is a multivariate problems that makes it very heterogeneous and difficult to quantity. Even though this has been studied for many decades, field studies that measure wave propagation and attenuation concurrently with mechanical sea ice properties are still needed in order to understand wave dispersion and processes responsible for wave attenuation.
— The subject of MIZ thermodynamics was purposely left aside in this review, but is nonetheless very important for MIZ dynamics and for understanding its role in the evolution of the polar climate in both hemispheres. For instance, frazil ice is currently left untreated by models as a mechanical entity and there are very few field and modelling studies on processes affecting frazil ice, especially in the presence of waves.

Data accessibility. Data for figure 3 are digital ice charts made available publicly by national ice services of Canada and Greenland, and the MATLAB code used to process them is available through Git (gitlab.uqar.ca/nicopa01/MIZ_width.git.).

Conflict of interest declaration. I declare I have no competing interests.

Funding. This work is funded by the Natural Sciences and Engineering Research Council of Canada through the Discovery Grant program (RGPIN-2019-06563) *Physics of Seasonal Sea Ice*.

Acknowledgements. I personally thank Luke Bennetts and the editors of the special issue for inviting me to write this review, and colleagues at Institut des sciences de la mer de Rimouski (ISMER) for valuable feedbacks on the manuscript. I thank Paul Nicot for making figure 3, Haijin Dai for giving its permission to use figure 1 and Amélie Bouchat for figure 4. Comments and suggestions made by the three reviewers were enormously useful and I wish to thank them all.

References

1. Overland JE, Wang M. 2013 When will the summer arctic be nearly sea ice free? *Geophys. Res. Lett.* **40**, 2097–2101. (doi:10.1002/grl.50316)
2. Shu Q, Wang Q, Song Z, Qiao F, Zhao J, Chu M, Li X. 2020 Assessment of sea ice extent in CMIP6 with comparison to observations and CMIP5. *Geophys. Res. Lett.* **47**, e2020GL087965. (doi:10.1029/2020GL087965)
3. Wang M, Overland JE. 2012 A sea ice free summer Arctic within 30 years: an update from CMIP5 models. *Geophys. Res. Lett.* **39**, L18501. (doi:10.1029/2012GL052868)
4. Hunke E *et al.* 2020 Should sea-ice modeling tools designed for climate research be used for short-term forecasting? *Curr. Clim. Change Rep.* **6**, 121–136. (doi:10.1007/s40641-020-00162-y)
5. Lemieux JF, Bouillon S, Dupont F, Flato G, Losch M, Rampal P, Tremblay LB, Vancoppenolle M, Williams T. 2017 Sea ice physics and modelling. In *Sea Ice Analysis and Forecasting: Towards an Increased Reliance on Automated Prediction Systems*. pp. 1–9. Cambridge, UK: Cambridge University Press. (doi:10.1017/9781108277600.003)
6. Johannessen OM, Johannessen JA, Morison J, Farrelly BA, Svendsen EAS. 1983 Oceanographic conditions in the marginal ice zone north of Svalbard in early Fall 1979 with an emphasis on mesoscale processes. *J. Geophys. Res.* **88**, 2755–2769. (doi:10.1029/JC088iC05p02755)

7. Shuchman RA, Burns BA, Johannessen OM, Josberger EG, Campbell WJ, Manley TO, Lannelongue N. 1987 Remote sensing of the Fram Strait marginal ice zone. *Science* **236**, 429–431. (doi:10.1126/science.236.4800.429)
8. McNutt L, Digby S, Carsey F, Holt B, Crawford J, Tang CL, Gray AL, Livingstone C. 1988 LIMEX'87: the Labrador Ice Margin Experiment, March 1987—a pilot experiment in anticipation of RADARSAT and ERS 1 data. *EOS Trans. Am. Geophys. Union* **69**, 634–643. (doi:10.1029/88EO00201)
9. Leppäranta M, Hibler III WD. 1985 The role of plastic ice interaction in marginal ice zone dynamics. *J. Geophys. Res.* **90**, 11 899–11 909. (doi:10.1029/JC090iC06p11899)
10. Røed LP, O'Brien JJ. 1983 A coupled ice-ocean model of upwelling in the marginal ice zone. *J. Geophys. Res.* **88**, 2863–2872. (doi:10.1029/JC088iC05p02863)
11. Dai H, Cui J, Yu J. 2017 Revisiting mesoscale eddy genesis mechanism of nonlinear advection in a marginal ice zone. *Acta Oceanol. Sin.* **36**, 14–20. (doi:10.1007/s13131-017-1134-8)
12. Squire VA, Dugan JP, Wadhams P, Rottier PJ, Liu AK. 1995 Of ocean waves and sea ice. *Ann. Rev. Fluid Mech.* **27**, 115–168. (doi:10.1146/annurev.fl.27.010195.000555)
13. Squire VA. 2007 Of ocean waves and sea-ice revisited. *Cold Reg. Sci. Tech.* **49**, 110–133. (doi:10.1016/j.coldregions.2007.04.007)
14. Squire VA. 2020 Ocean wave interactions with sea ice: a reappraisal. *Ann. Rev. Fluid Mech.* **52**, 37–60. (doi:10.1146/annurev-fluid-010719-060301)
15. Thomson J. 2022 Wave propagation in the marginal ice zone: connections and feedback mechanisms within the air–ice–ocean system. *Phil. Trans. R. Soc. A* **380**, 20210251. (doi:10.1098/rsta.2021.0251)
16. Dai HJ, McWilliams JC, Liang JH. 2019 Wave-driven mesoscale currents in a marginal ice zone. *Ocean Model.* **134**, 1–17. (doi:10.1016/j.ocemod.2018.11.006)
17. Dumont D, Kohout A, Bertino L. 2011 A wave-based model for the marginal ice zone including a floe breaking parameterization. *J. Geophys. Res.* **116**, C04001. (doi:10.1029/2010JC006682)
18. Herman A. 2022 Granular effects in sea ice rheology in the marginal ice zone. *Phil. Trans. R. Soc. A* **380**, 20210260. (doi:10.1098/rsta.2021.0260)
19. Rothrock DA, Thorndike AS. 1984 Measuring the sea ice floe size distribution. *J. Geophys. Res.* **89**, 6477–6486. (doi:10.1029/JC089iC04p06477)
20. Toyota T, Takatsuji S, Nakayama M. 2006 Characteristics of sea ice floe size distribution in the seasonal ice zone. *Geophys. Res. Lett.* **33**, L02616. (doi:10.1029/2005GL024556)
21. Horvat C. 2022 Floes, the marginal ice zone and coupled wave-sea-ice feedbacks. *Phil. Trans. R. Soc. A* **380**, 20210252. (doi:10.1098/rsta.2021.0252)
22. Strong C, Rigor IG. 2013 Arctic marginal ice zone trending wider in summer and narrower in winter. *Geophys. Res. Lett.* **40**, 4864–4868. (doi:10.1002/grl.50928)
23. Rolph RJ, Feltham DL, Schröder D. 2020 Changes of the arctic marginal ice zone during the satellite era. *Cryosphere* **14**, 1971–1984. (doi:10.5194/tc-14-1971-2020)
24. Stroeve JC, Jenouvrier S, Campbell GG, Barbraud C, Delord K. 2016 Mapping and assessing variability in the Antarctic marginal ice zone, pack ice and coastal polynyas in two sea ice algorithms with implications on breeding success of snow petrels. *Cryosphere* **10**, 1823–1843. (doi:10.5194/tc-10-1823-2016)
25. Vichi M. 2021 A statistical definition of the Antarctic marginal ice zone. *Cryosphere Discuss.* 1–23. (doi:10.5194/tc-2021-307). Preprint.
26. Hakkinen S. 1987 Feedback between ice flow, barotropic flow, and baroclinic flow in the presence of bottom topography. *J. Geophys. Res.* **92**, 3807–3820. (doi:10.1029/JC092iC04p03807)
27. Hakkinen S. 1986 Coupled ice-ocean dynamics in the marginal ice zones, upwelling/downwelling and eddy generation. *J. Geophys. Res.* **91**, 819–832.
28. Häkkinen S. 1987 A coupled dynamic-thermodynamic model of an ice-ocean system in the marginal ice zone. *J. Geophys. Res.* **92**, 9469–9478. (doi:10.1029/JC092iC09p09469)
29. Manucharyan GE, Thompson AF. 2017 Submesoscale sea ice-ocean interactions in marginal ice zones. *J. Geophys. Res.* **122**, 9455–9475. (doi:10.1002/2017JC012895)
30. Liu AK, Häkkinen S, Peng CY. 1993 Wave effects on ocean-ice interaction in the marginal ice zone. *J. Geophys. Res.* **98**, 10 025–10 036. (doi:10.1029/93JC00653)

31. Ardhuin F, Collard F, Chapron B, Girard-Ardhuin F, Guitton G, Mouche A, Stopa JE. 2015 Estimates of ocean wave heights and attenuation in sea ice using the SAR wave mode on Sentinel-1A. *Geophys. Res. Lett.* **42**, 2317–2325. (doi:10.1002/2014GL062940)
32. Liu J, Scott KA, Fieguth PW. 2019 Detection of marginal ice zone in Synthetic Aperture Radar imagery using curvelet-based features: a case study on the Canadian East Coast. *J. Appl. Remote Sens.* **13**, 1–14. (doi:10.1117/1.JRS.13.014505)
33. Wadhams P, Holt B. 1991 Waves in frazil and pancake ice and their detection in Seasat synthetic aperture radar imagery. *J. Geophys. Res.* **96**, 8835–8852. (doi:10.1029/91JC00457)
34. Schulz-Stellenfleth J, Lehner S. 2002 Spaceborne synthetic aperture radar observations of ocean waves traveling into sea ice. *J. Geophys. Res.* **107**, 20-1–20-19. (doi:10.1029/2001JC000837)
35. Ardhuin F *et al.* 2017 Measuring ocean waves in sea ice using SAR imagery: a quasi-deterministic approach evaluated with Sentinel-1 and in-situ data. *Remote Sens. Environ.* **189**, 211–222. (doi:10.1016/j.rse.2016.11.024)
36. Stopa JE, Sutherland P, Ardhuin F. 2018 Strong and highly variable push of ocean waves on Southern Ocean sea ice. *Proc. Natl Acad. Sci.* **115**, 5861–5865. (doi:10.1073/pnas.1802011115)
37. Horvat C, Blanchard-Wrigglesworth E, Petty A. 2020 Observing waves in sea ice with ICESat-2. *Geophys. Res. Lett.* **47**, e2020GL087629. (doi:10.1029/2020GL087629)
38. Brouwer J *et al.* 2022 Altimetric observation of wave attenuation through the Antarctic marginal ice zone using ICESat-2. *Cryosphere* **16**, 2325–2353. (doi:10.5194/tc-16-2325-2022)
39. Liu AK, Martin S, Kwok R. 1997 Tracking of ice edges and ice floes by wavelet analysis of SAR images. *J. Atmos. Ocean. Tech.* **14**, 1187–1198. (doi:10.1175/1520-0426(1997)014<1187:TOIEAI>2.0.CO;2)
40. Soh LK, Tsatsoulis C, Holt B. 1998 Identifying ice floes and computing ice floe distributions in SAR images. In *Analysis of SAR Data of the Polar Oceans* (eds C Tsatsoulis, R Kwok), pp. 9–34. Berlin; Heidelberg: Springer. (doi:10.1007/978-3-642-60282-5_2)
41. Simard B *et al.* 2005 *Manual of standard procedures for observing and reporting ice conditions (MANICE)*. 9th edn. Ottawa, Canada: Meteorological Service of Canada.
42. Williams TD, Bennetts LG, Squire VA, Dumont D, Bertino L. 2013 Wave-ice interactions in the marginal ice zone. Part 2: numerical implementation and sensitivity studies along 1D transects of the ocean surface. *Ocean Model.* **71**, 92–101. (doi:10.1016/j.ocemod.2013.05.011)
43. Untersteiner N, Thorndike AS, Rothrock D, Hunkins K. 2007 AIDJEX revisited: a look back at the U.S.-Canadian Arctic Ice Dynamics Joint Experiment 1970–78. *Arctic* **60**, 327–336.
44. Lüpkes C, Birnbaum M. 2005 Surface drag in the Arctic marginal sea-ice zone: a comparison of different parameterisation concepts. *Bound.-Layer Meteorol.* **117**, 179–211. (doi:10.1007/s10546-005-1445-8)
45. Tsamados M, Feltham DL, Schroeder D, Flocco D, Farrell SL, Kurtz N, Laxon SW, Bacon S. 2014 Impact of variable atmospheric and oceanic form drag on simulations of Arctic sea ice. *J. Phys. Oceanogr.* **44**, 1329–1353. (doi:10.1175/JPO-D-13-0215.1)
46. Brenner S, Rainville L, Thomson J, Cole S, Lee C. 2021 Comparing observations and parameterizations of ice-ocean drag through an annual cycle across the Beaufort Sea. *J. Geophys. Res.* **126**, e2020JC016977. (doi:10.1029/2020JC016977)
47. Lemieux JF, Tremblay LB, Dupont F, Plante M, Smith GC, Dumont D. 2015 A basal stress parameterization for modeling landfast ice. *J. Geophys. Res.* **120**, 3157–3173. (doi:10.1002/2014JC010678)
48. Thorndike AS, Rothrock DA, Maykut GA, Colony R. 1975 The thickness distribution of sea ice. *J. Geophys. Res.* **80**, 4501–4513. (doi:10.1029/JC080i033p04501)
49. Steele M. 1992 Sea ice melting and floe geometry in a simple ice-ocean model. *J. Geophys. Res.* **97**, 17 729–17 738. (doi:10.1029/92JC01755)
50. Zhang J, Schweiger A, Steele M, Stern H. 2015 Sea ice floe size distribution in the marginal ice zone: theory and numerical experiments. *J. Geophys. Res.* **120**, 3484–3498. (doi:10.1002/2015JC010770)
51. Horvat C, Tziperman E. 2015 A prognostic model of the sea-ice floe size and thickness distribution. *Cryosphere* **9**, 2119–2134. (doi:10.5194/tc-9-2119-2015)
52. Dolatshah A, Nelli F, Bennetts LG, Alberello A, Meylan MH, Monty JP, Toffoli A. 2018 Letter: hydroelastic interactions between water waves and floating freshwater ice. *Phys. Fluids* **30**, 091702. (doi:10.1063/1.5050262)

53. Dumas-Lefebvre E, Dumont D. 2021 Aerial observations of sea ice break-up by ship waves. *Cryosphere Discuss.* **2021**, 1–26. (doi:10.5194/tc-2021-328)
54. Roach LA, Horvat C, Dean SM, Bitz CM. 2018 An emergent sea ice floe size distribution in a global coupled ocean-sea ice model. *J. Geophys. Res.* **123**, 4322–4337. (doi:10.1029/2017JC013)
55. Hall RT, Rothrock DA. 1987 Photogrammetric observations of the lateral melt of sea ice floes. *J. Geophys. Res.* **92**, 7045–7048. (doi:10.1029/JC092iC07p07045)
56. Hibler III WD. 1979 A dynamic thermodynamic sea ice model. *J. Phys. Oceanogr.* **9**, 815–846.
57. Hibler III WD. 1977 A viscous sea ice law as a stochastic average of plasticity. *J. Geophys. Res.* **82**, 3932–3938. (doi:10.1029/JC082i027p03932)
58. Bouchat A, Tremblay B. 2017 Using sea-ice deformation fields to constrain the mechanical strength parameters of geophysical sea ice. *J. Geophys. Res.* **122**, 5802–5825. (doi:10.1002/2017JC013020)
59. Hošeková L, Eidam E, Panteleev G, Rainville L, Rogers WE, Thomson J. 2020 Landfast ice and coastal wave exposure in northern Alaska. *Geophys. Res. Lett.* **6**, 121–136. (doi:10.1007/s40641-020-00162-y)
60. Herman A, Wenta M, Cheng S. 2021 Sizes and shapes of sea ice floes broken by waves—a case study from the east Antarctic coast. *Front. Earth Sci.* **9**, 655977. (doi:10.3389/feart.2021.655977)
61. Shen HH, Hibler III WD, Leppäranta M. 1986 On applying granular flow theory to a deforming broken ice field. *Acta Mech.* **63**, 143–160. (doi:10.1007/BF01182545)
62. Shen HH, Hibler III WD, Leppäranta M. 1987 The role of floe collisions in sea ice rheology. *J. Geophys. Res.* **92**, 7085–7096. (doi:10.1029/JC092iC07p07085)
63. Jop P, Forterre Y, Pouliquen O. 2006 A constitutive law for dense granular flows. *Nature* **441**, 727–730. (doi:10.1038/nature04801)
64. Feltham DL. 2005 Granular flow in the marginal ice zone. *Phil. Trans. R. Soc. A* **363**, 1677–1700. (doi:10.1098/rsta.2005.1601)
65. Longuet-Higgins MS, Stewart RW. 1964 Radiation stresses in water waves; a physical discussion, with applications. *Deep Sea Res. Oceanogr. Abstr.* **11**, 529–562. (doi:10.1016/0011-7471(64)90001-4)
66. Longuet-Higgins M. 1977 The mean forces exerted by waves on floating or submerged bodies with applications to sand bars and wave power machines. *Proc. R. Soc. Lond. A* **352**, 463–480. (doi:10.1098/rspa.1977.0011)
67. Sutherland P, Dumont D. 2018 Marginal ice zone thickness and extent due to wave radiation stress. *J. Phys. Oceanogr.* **48**, 1885–1901. (doi:10.1175/JPO-D-17-0167.1)
68. Hopkins MA, Tuhkuri J. 1999 Compression of floating ice fields. *J. Geophys. Res.* **104**, 15 815–15 825. (doi:10.1029/1999JC900127)
69. Dai M, Shen HH, Hopkins MA, Ackley SF. 2004 Wave rafting and the equilibrium pancake ice cover thickness. *J. Geophys. Res.* **109**, C07023. (doi:10.1029/2003JC002192)
70. Uzuner MS, Kennedy JF. 1976 Theoretical model of river ice jams. *J. Hydraul. Div.* **102**, 1365–1383. (doi:10.1061/JYCEAJ.0004618)
71. Auclair J-P, Dumont D, Lemieux J-F, Ritchie H. 2022 A model study of convergent dynamics in the marginal ice zone. *Phil. Trans. R. Soc. A* **380**, 20210261. (doi:10.1098/rsta.2021.0261)
72. Auclair JP, Lemieux JF, Tremblay LB, Ritchie H. 2017 Implementation of Newton's method with an analytical Jacobian to solve the 1D sea ice momentum equation. *J. Comput. Phys.* **340**, 69–84. (doi:10.1016/j.jcp.2017.02.065)
73. Williams TD, Rampal P, Bouillon S. 2017 Wave–ice interactions in the neXtSIM sea-ice model. *Cryosphere* **11**, 2117–2135. (doi:10.5194/tc-11-2117-2017)
74. Olason E, Boutin G, Korosov A, Rampal P, Williams T, Dansereau V, Samaké A. 2022 A new brittle rheology and numerical framework for large-scale sea-ice models. *JAMES*, 1–35. Preprint. (doi:10.1002/essoar.10507977.1)
75. Hopkins MA, Hibler III WD, Flato GM. 1991 On the numerical simulation of the sea ice ridging process. *J. Geophys. Res.* **96**, 4809–4820. (doi:10.1029/90JC02375)
76. Boutin G, Williams T, Rampal P, Olason E, Lique C. 2021 Wave–sea-ice interactions in a brittle rheological framework. *Cryosphere* **15**, 431–457. (doi:10.5194/tc-15-431-2021)
77. Petty AA, Bagnardi M, Kurtz NT, Tilling R, Fons S, Armitage T, Horvat C, Kwok R. 2021 Assessment of ICESat-2 sea ice surface classification with sentinel-2 imagery: implications for freeboard and new estimates of lead and floe geometry. *Earth Space Sci.* **8**, e2020EA001491. (doi:10.1029/2020EA001491)